

Diagnostics of ultra-thin tungsten films on silicon substrate using atomic force microscopy

Milan Navrátil, Vojtěch Křesálek, František Hruška, Tomáš Martínek, Josef Kudělka and Jaroslav Sobota

Abstract— In this article, atomic force microscopy method was used for diagnostics of ultra-thin tungsten films which were deposited on silicon substrate. Radio frequency magnetron sputtering method was used for tungsten deposition on the surface. According to atomic forces between the tip and the sample, topographical structures were measured and imaged.

Keywords— atomic force microscopy, scanning microwave microscopy, tungsten on silicon substrate, ultra-thin film.

I. INTRODUCTION

NOWADAYS, with development of electronics and microelectronics the complexity of electronic devices increases approximately four times every three years. The smallest structure size decreases with ratio 0.5 in the same period. During this integration rising the physical limits of electron motion in electric field must be taken into account. For that reason, leading world producers invest into development of electronic structures and networks in nano-scale. The boundary between micro and nano systems is about 10 nm, where classical physical laws are not valid anymore and quantic physics begins to be applied. Near this area, ultra-thin (<100 nm) metal films, except others, play important role in industry, e.g., electrical components fabrication as a diffusion barrier [1]. They prevent from undesirable diffusion of dopants and interlayer diffusion interactions. The thin films are typically used for a dielectric of a semi-conductor devices, transparent conductors of a liquid-crystal display, or protective layer of an electroluminescent thin film display. Moreover, these components are used in modern sensor construction, spin electronics, radiographic optics and nanomaterial, e.g. smart mirrors for solar energy [2].

Measuring methods and capabilities for technology verification of these components or their characterization are

limited due to their structure size which is often in atomic or sub-atomic resolution. There are only few possible measuring methods – diffraction techniques, scanning transmission electron microscopy (STEM) and atomic force microscopy (AFM). These methods are commonly used for polycrystallinity confirmation and characterization of nanostructures and allows using different imaging modes. They bring cons and pros, depending on matter of investigation. In the literature some papers have been published which describe measuring methods of thin metal films, but the thicknesses are greater than tens of nanometers [3].

Tungsten oxide (WO_3) has been broadly studied due to its unique electro-optical, electric, ferroelectric properties which may correspond to crystal structure. Nevertheless, the ideal cubic structure does not appear in bulk samples of WO_3 . For ultra-thin tungsten films with thicknesses less than 10 nm, a cubic modification of WO_3 has been reported [4]. Deposition of tungsten film can be executed in many different methods based on, for example, radio frequency sputtering, thermal evaporation, chemical vapor, pulsed-laser method and sol-gel method [5].

In our case, two methods of scanning probe microscopy based on different tip-sample interaction were used for diagnostician of the ultra-thin tungsten films on silicon substrates – atomic force microscopy and scanning microwave microscopy (SMM). With these methods we can concurrently get both topographical and some electromagnetic properties of the analyzed sample. It was not clear if the metal-like conductivity of ultra-thin tungsten layer proves or not, despite some paper investigated the surface structure and electrical conductivity of WO_3 thin films on other substrates [6]. For that reason, we decided to use scanning microwave method for verification of homogeneity of sputtered layer of tungsten.

II. SCANNING PROBE MICROSCOPY

Scanning probe microscopy (SPM) devices operate on a completely different principle than conventional microscopic techniques. This technique was firstly used in 1981 – scanning tunneling microscope (STM) [7]. In general, SPM images are obtained by positioning the mechanical probe close to the sample surface. The probe measures any interaction between probe and the sample surface and creates feedback signal, which is used for vertical positioning of the probe (axis z) with resolution of the order of 10^{-10} nanometers. Position of the probe above sample is controlled with piezoelectric system

The authors gratefully acknowledge financial support from Ministry of Education, Youth and Sports of the Czech Republic (CEBIA-Tech No. CZ.1.05/2.1.00/03.0089) and (LO1212) together with the European Commission (ALISI No. CZ.1.05/2.1.00/01.0017).

M. Navrátil, V. Křesálek, F. Hruška, T. Martínek and J. Kudělka are with the Tomas Bata University in Zlín, Faculty of Applied Informatics, nám. T.G.Masaryka 5555, 760 05 Zlín, CZECH REPUBLIC (phone: +420-57-603-5283, fax: +420-57-603-5279, email: {navratil, kresalek, hruska, tmartinek, kudelka}@fai.utb.cz).

J. Sobota is with the Academy of Sciences of the Czech Republic, Institute of Scientific Instruments, Královopolská 147, 612 64 Brno, CZECH REPUBLIC (email: sobota@isibrno.cz)

according to chosen scan grid (axis x-y), see Fig. 1. Final scan image is put together via computer processing.

There can be two ways how to perform SPM measurement. Mode with constant height keeps the distance the same between tip and sample during the measurement, the magnitude of interaction is measured. This requires rather very flat surfaces due to possible damage of the probe or the sample. In mode of constant interaction, the distance is controlled via feedback which tries to keep the same interaction value. This approach is slower, but it allows to detect larger changes in sample profile [8].

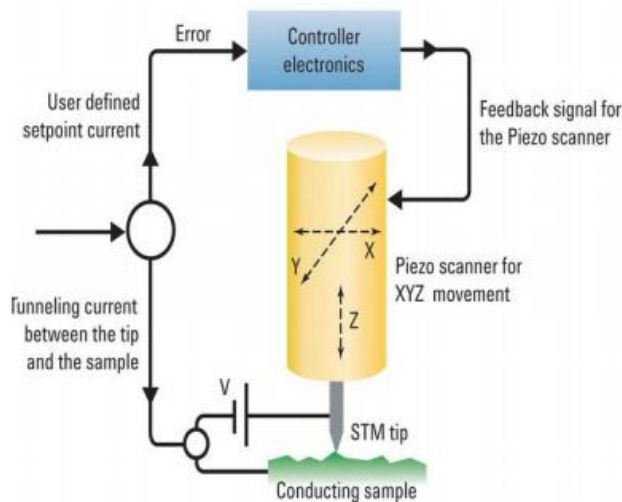


Fig. 1 Scanning probe microscopy principle (involving STM) [9]

A. Atomic force microscopy

Atomic force microscopy is a derived method from scanning probe microscopy where intermolecular forces are measured over the sample surface. These forces are induced with immediate approach ($\sim 2\text{\AA}$ to 20\AA) of the AFM tip to sample surface. Resultant force can be either attractive or repulsive, depending on distance, and it causes bend of cantilever with the tip, see Fig. 2.

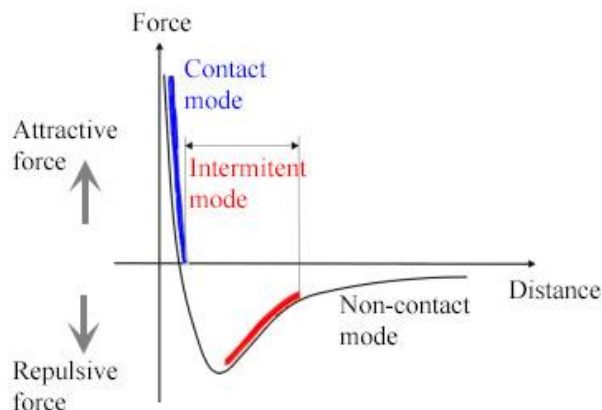


Fig. 2 Dependence of resulting force vs distance

These slight changes in position are detected with sensitive device. It usually consists of laser diode and four segment photodiode. Laser beam is focused on the cantilever end where is reflected to the photo detector from. During movement of the cantilever the energy is not uniformly spread

into all quadrants, see Fig. 3. From these energy changes in vertical axis the deflection can be detected. From horizontal axis the torsion can be measured.

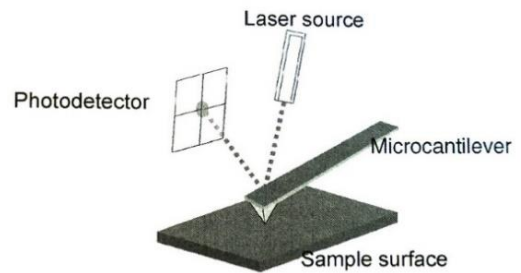


Fig. 3 AFM detection principle [10]

According to tip-sample distance there is measuring in three modes. The first one is contact mode, the distance is so small that the cantilever is deflected from the sample surface. Force is on the order of 10^{-7} N. The second one is non-contact mode, where van der Waals forces affect (on the order of 10^{-12} N). The cantilever is attracted to sample, but forces are very small and the bend is small as well. In order to improve sensitivity, the cantilever is oscillated near its resonant frequency with given amplitude (on the order of 10^{-9} m). Changes in resonant frequency during tip approach is detected and evaluated. The last one is tapping mode, which is very similar to previous one, but the amplitude is proportional to intermittent contact between tip and sample.

All mentioned modes have pros and cons, depending on type of the sample (soft or hard matters, liquids, air, and vacuum etc.) [11].

B. Scanning microwave microscopy

Scanning microwave microscopy (SMM) is a derived method of SPM that combines the electromagnetic measurement capabilities of a microwave vector network analyzer (VNA) with the nanometer resolution and Angstrom-scale positioning capabilities of classical AFM [12]. This measurement method allows calibrated measurements of electrical properties such as impedance and capacitance, with the high spatial resolution [13].

Impedance can be measured in three different ways, according to the frequency and the magnitudes involved. VNA measures impedance of a device under test (DUT) by comparing the reflected signal to the incident signal. This method of measuring impedance is the one that works best at the microwave frequencies and for impedance values at or near the characteristic impedance of transmission lines (50 or $75\ \Omega$). DUT is represented by interface AFM tip – sample surface. Relation between signal magnitudes and DUT's impedance is as follows

$$\frac{U_{reflected}}{U_{incident}} = \Gamma = \frac{Z_L - Z_0}{Z_L + Z_0} = |\Gamma| e^{j\varphi} \quad (1)$$

where Γ is reflection coefficient. The incident microwave signal (on the order of 10^9 Hz) travels through a series of components before it reaches the tip-sample interface by means of a transmission line with characteristic impedance Z_0 ($50\ \Omega$).

The impedance mismatch between the transmission line and the DUT causes the incident microwave signal to partially reflect from the tip-sample interface back towards the stimulus signal source inside the VNA. This reflected signal is proportional to the impedance mismatch. The incident microwave signal and the reflected microwave signal together contain information about DUT's impedance Z_L .

When the value of Z_L is close to that of Z_0 , the plot has the steepest slope, which corresponds to the highest sensitivity and the highest resolution. In our case, Z_0 is 50Ω , but Z_L is generally not near this value.

The accuracy of a VNA impedance measurement reduces however as the impedance values move away from these characteristic values.

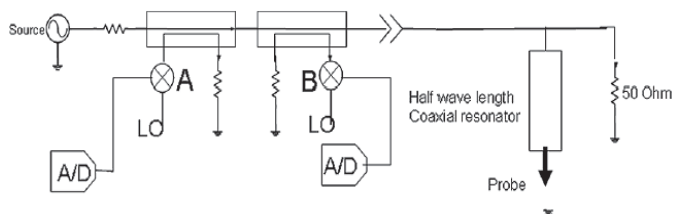


Fig. 4 Scheme of measuring principle of SMM

In order to bring the value of Z_L closer to that of Z_0 and therefore exploit the VNA's impedance measurement capability in its most accurate and sensitive range, the SMM uses a half-wavelength impedance transformer to place the measurand — the DUT — directly across an external 50Ω impedance, that is, parallel to it, it is evident from Fig. 4. This configuration enables measuring with a very high resolution the small changes of a very small impedance. Considering the relation

$$Z_L = \frac{1}{\omega C} \quad (2)$$

we can get capacitance changes on the order of 10^{-19} F across a 10^{-16} F base capacitance of dielectric samples. The AFM tip is metalized and in contact with the sample surface. If this surface is semiconducting with thin oxide layer, the interface tip – sample forms MOS capacitor. The higher frequencies in SMM lead to better sensitivity and resolution for measuring the tip-sample capacitance [14].

III. EXPERIMENTAL

A. Deposition of ultra-thin films of tungsten on silicon substrate

Tungsten coatings was deposited in a Leybold Z550 sputtering unit using 150 mm tungsten cathode 99.95% in purity. The argon flux was regulated with high accuracy by mass-flow controller. Argon deposition pressure was held on 200 mPa. Films were deposited in the radio-frequency (RF) mode at a power of 150 W, and the distance between the target and the rotating substrate holder 48 mm was held constant [15].

Substrate oscillates under the magnetron, and during one eight second lasting oscillation 0.3 nm thick layer was

deposited. The thicknesses of the tungsten layers were calculated from Taylor-Hobson profilometer measurement on coatings deposited during hundred eight second lasting oscillations at the conditions given above.



Fig. 5 Leybold Z550 sputtering unit



Fig. 6 Substrate oscillates under the magnetron, and during one 8 s lasting oscillation 0.3 nm thick layer was deposited

Two types of silicon substrate were prepared. Silicon wafer with thickness of 200 nm layer of SiO_2 (substrate marked as SW200), and silicon wafer with thickness approximately of 1 up to 2 nm of native silicon dioxide (substrate marked as SW2). Mentioned thickness range depends on temperature and length of sample storage. On surface of these substrates ultra-thin films of tungsten were deposited with different thicknesses (TH0 with no tungsten, TH3 with thickness of 0.3 nm, TH6 with thickness of 0.6 nm).

Prepared samples were stored at room temperature in common laboratory condition, so that we expect oxidation of the tungsten film.

B. Sample preparation and measurement

Surfaces of all measured samples were carefully rinsed with isopropyl alcohol and then dried out. No other special preparation was used. Measurement was performed with

atomic force microscope Agilent 5420 in free air on common laboratory conditions. Microwave vector network analyzer PNA N5230A providing microwave signal 1.5 – 6 GHz was used. SMM, in our case frequency of 2.415235 GHz. All metal (Pt-Ir) AFM probe (size 400 x 60 μm) with spring constant of 0.3 N/m, resonant frequency of 4.5 kHz and with diameter less than 7 nm was used.

Measurement area of 4 μm x 4 μm was chosen for all analyzed samples. Measurement was gradually accomplished at three different locations of sample surface. AFM topography, SMM amplitude and capacity of samples was measured and some of obtained results were visualized using PicoView and PicoImage basic software [16].

Another data processing leading to determination of profile measurement at chosen locations, mean diameter of surface structures, their mean height has been also done.

IV. RESULTS AND DISCUSSIONS

Topography characterization of sample SW200 without tungsten (Fig. 7a) film has been accomplished where flat surface was expected.

Some structures with mean height of four nanometers and mean diameter of 500 nm were observed. It could be dirt rather than surface failure. Analysis of sample SW200 with sputtered 0.3 thickness of tungsten showed very gentle blobs with mean height of 25 nm, mean diameter of 50 nm (Fig. 7b). Results of the thickest tungsten film showed the objects with mean height of 24 nm and mean diameter of 510 nm, as can be seen in Fig. 7c.

Some of the typical structured objects can be seen in topography profiles taken at different locations of analyzed sample, see Fig. 8. Results of concurrently measured SW200 sample using SMM method have not provided any relevant or reproducible information.

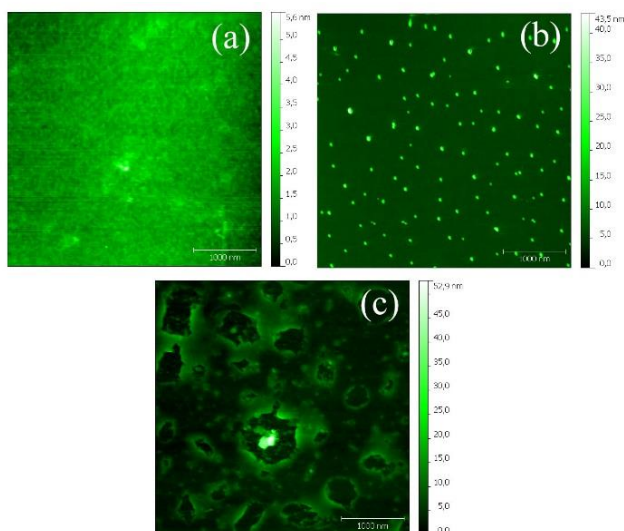


Fig. 7 Sample SW200: 2D topography image from AFM method. (a) – no tungsten, (b) – 0.3 nm tungsten film, (c) – 0.6 nm tungsten film.

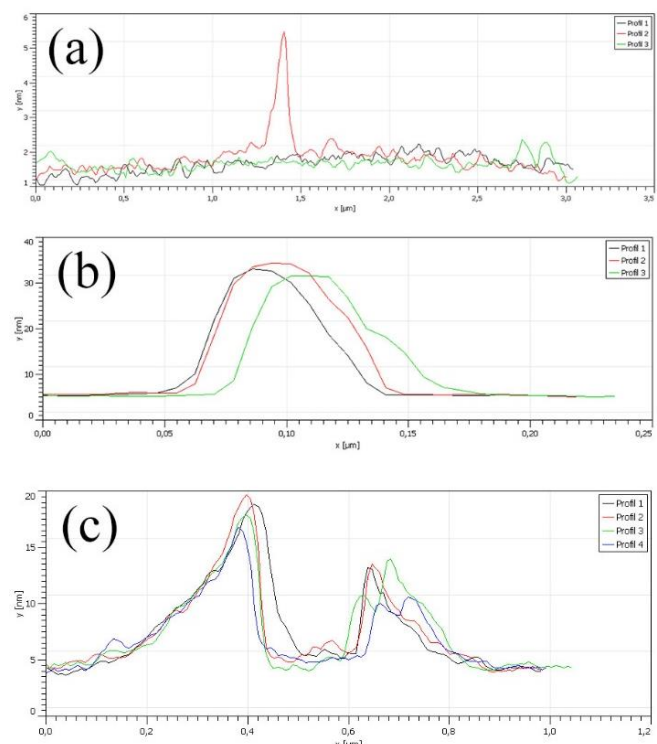


Fig. 8 Illustration of typical structures in topographical profiles of SW200 samples. (a) – no tungsten, (b) – 0.3 nm tungsten film, (c) – 0.6 nm tungsten film

The same analysis has been done for samples with ultra-thin native layer of silicon dioxide (SW2). From the topographical point of view, there were no significant changes. The results have seen similar to samples SW200 except sample with tungsten film of 0.3 nm thickness. The mean diameter is approximately eight times greater while mean height is half, see Fig. 9 and Fig. 10. This flattening can be in relation with oxidation process of the tungsten. To understand problem with oxidation, it is necessary to measure the sample in vacuum and study whole oxidation process including its kinetics.

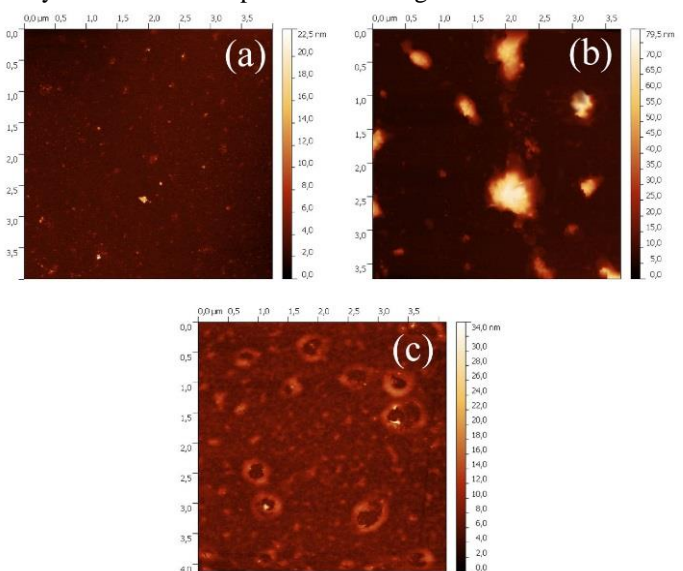


Fig. 9 Sample SW2: 2D topography image from AFM method. (a) – no tungsten, (b) – 0.3 nm tungsten film, (c) – 0.6 nm tungsten film.

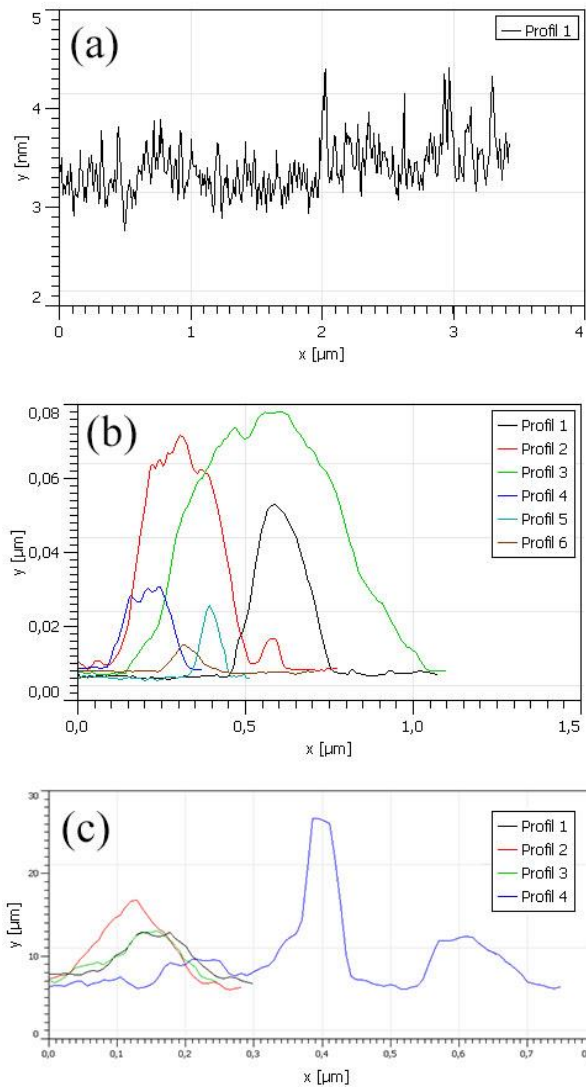


Fig. 10 Illustration of typical structures in topographical profiles of SW2 samples. (a) – no tungsten, (b) – 0.3 nm tungsten film, (c) – 0.6 nm tungsten film

Mentioned results were presented from 2-D point of view. Used software Pico Image Basic allowed us to make visual representation in 3-D appearance. Following results are related to the sample of silicon wafer with thickness approximately of 1 up to 2 nm of native silicon dioxide.

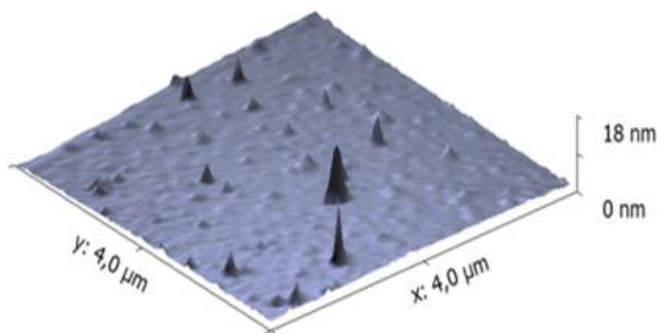


Fig. 11 3-D visualization of SW2 sample without tungsten film.

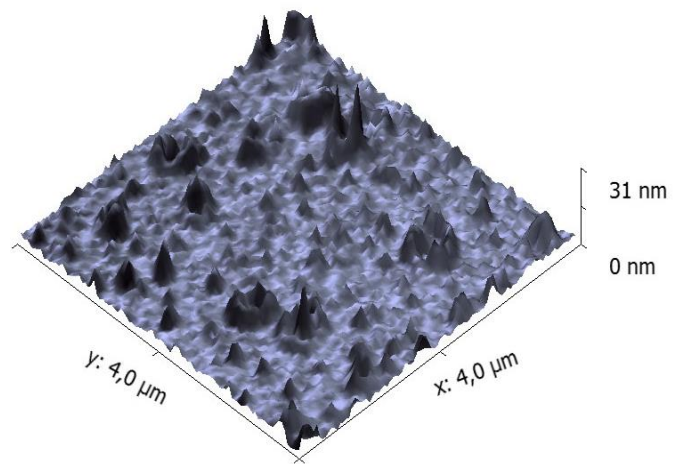


Fig. 12 3-D visualization of SW2 sample where thickness of tungsten film is 0.3 nm.

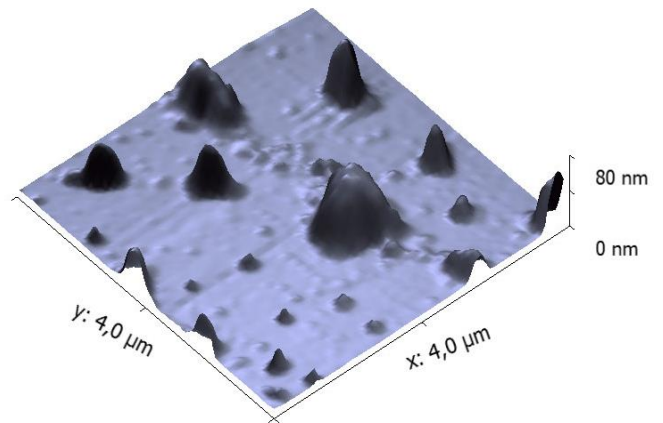


Fig. 13 3-D visualization of SW2 sample where thickness of tungsten film is 0.6 nm.

The same analysis was accomplished for samples of silicon wafer with thickness of 200 nm layer of SiO₂.

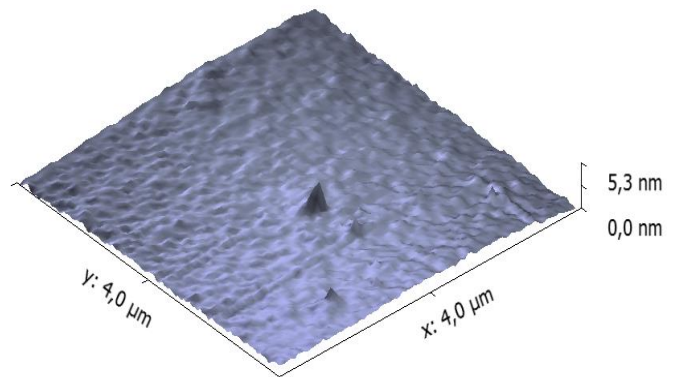


Fig. 14 3-D visualization of SW200 sample without tungsten film.

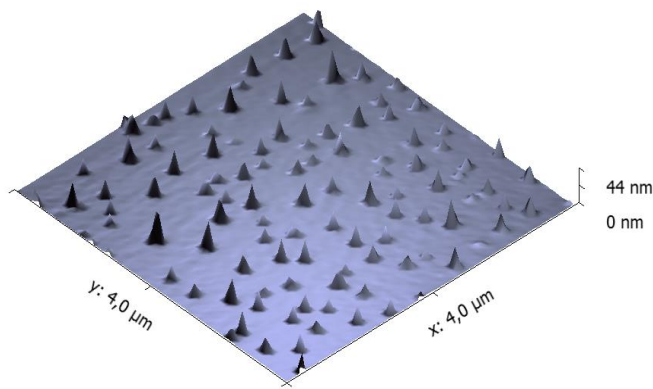


Fig. 15 3-D visualization of SW200 sample where thickness of tungsten film is 0.3 nm..

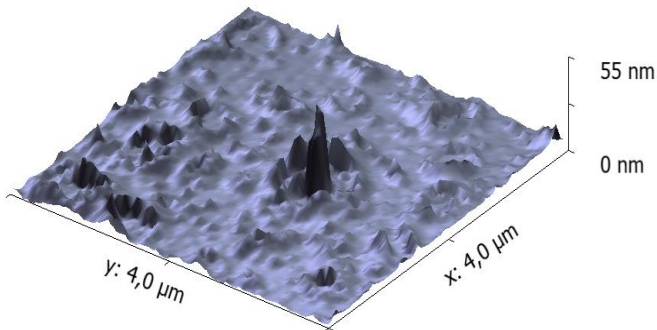


Fig. 16 3-D visualization of SW200 sample where thickness of tungsten film is 0.6 nm.

Summarized topographical information about analyzed ultra-thin tungsten films of different thicknesses on silicon substrate can be seen in Table I. Moreover, there is also calculation of sample area (expressed in percentage) which fulfils condition given by minimal structure height (threshold in nanometers). This information was acquired with software Gwyddion, in Fig. 17 there is an illustration of grain analysis according to given threshold value. Another statistical calculations were also done in this software.

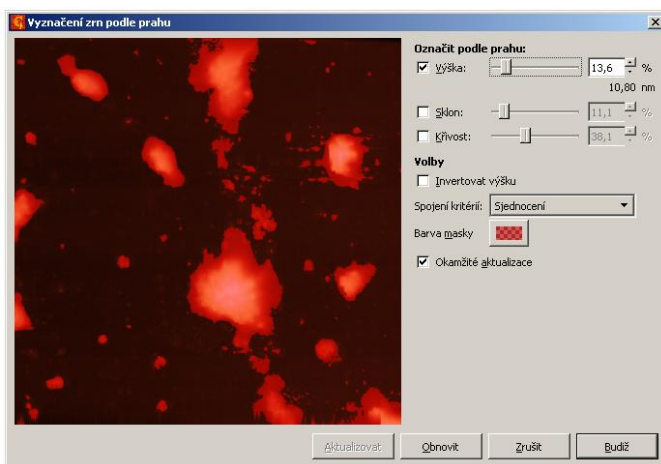


Fig. 17 Grain analysis and statistical evaluation in software Gwyddion.

Table I Statistical evaluation of topographical properties of measured structures

Analyzed sample	Mean Height / Diameter [nm]	Threshold [nm]	Threshold structures area [%]
WS200_TH0	4 / 500	2.5	0.6
WS200_TH3	25 / 50	6.5	4.2
WS200_TH6	24 / 510	6.5	21.4
WS2_TH0	12 / 350	2.5	0.5
WS2_TH3	13 / 410	10.8	16.7
WS2_TH6	23 / 480	10.8	30

Some results of concurrently measured samples on substrate with native silicon dioxide using SMM method are depicted in Fig. 18. The changes in amplitude (a) are shown, there are some structures of oval shapes which are resemble objects from topography interpretation. They correspond to smaller objects size which were acquired with AFM method.

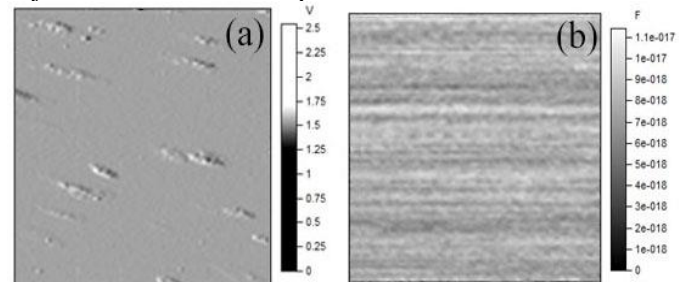


Fig. 18. SMM image – sample SW2_TH3, changes in amplitude of microwave signal (a) and changes in capacitance of the tip-sample interface (b).

On the other hand, capacitance changes are observable on the order of attofarads, see illustration in Fig. 18 (b). This results would indicate that the layer is conductive and homogeneous. There is a need to use another electric method, moreover with higher spatial resolution, such as scanning tunneling microscopy to verify conductivity of ultra-thin tungsten film.

V. CONCLUSION

Characterization of ultra-thin tungsten layer on silicon substrates was demonstrated using the two methods of scanning probe microscopy. Classical atomic force microscopy has showed the potential this method for studying of ultra-thin film structures, thicknesses and offered superficial insight into the oxidation process of tungsten on various silicon substrates. As it has not been clear, if the metal-like conductivity of ultra-thin tungsten layer proves or not, we have expected that SMM could answer that problem. From this reason, scanning microwave microscopy was used for homogeneity verification of ultra-thin sputtered layers. Interpretation of SMM results have indicated that sample with tungsten film with minimal thickness of 0.3 nm could be homogeneous. However, this opinion should be confirmed and proved with measuring of more samples. From the statistical point of view, it will be necessary to prepare samples over

larger range of ultra-thin tungsten thicknesses. According to all obtained results, the method of scanning tunneling microscopy (STM) would be more appropriate. Moreover, the spatial resolution of STM is generally higher than SMM, which is given by principle of the method.

REFERENCES

- [1] I. Fernandez, X. Borris and F. Pérez-Murano, "Atomic force microscopy local oxidation of silicon nitride thin films for mask fabrication", *Nanotechnology*, vol 16, no. 11, pp. 2731–2737, Nov. 2005.
- [2] C. M. Lampert, "Smart switchable glazing for solar energy", *Solar Energy Materials and Solar Cells.*, no. 52, pp. 207–221, 1998.
- [3] F. Houzé et al. "Imaging the local electrical properties of metal surfaces by atomic force", *Applied physics letters*. 1996.
- [4] E. Salje, "The orthorhombic phase of WO₃", *Acta Crystallographica*, vol. B33, pp. 574–577, 1977.
- [5] J. W. Klaus, S. J. Ferro and S. M. George, "Atomic layer deposition of tungsten using sequential surface chemistry", *Thin Solid Films*, no. 360, pp. 145–153, 2000.
- [6] M. Gillet et al., "The structure and electrical conductivity of vacuum-annealed WO₃ thin films", *Thin Solid Films*, vol. 467 (1-2), pp. 239–246 2004.
- [7] G. Binnig and H. Rohrer, "Scanning tunneling microscopy", *Helvetica Physica Acta*, no.. 55, pp. 726-735, 1982.
- [8] P. Hawkens and J. C. H. Spence, *Science of microscopy*, Springer, 2008, pp. 929-969.
- [9] Agilent Technologies. *5420 Scanning Probe Microscope: Users guide* [online]. USA, 2012. Available: http://nano.tm.agilent.com/PDFs/5420_User_Guide_Revision_D.pdf
- [10] V. Tsukruk V. and S. Singamaneni, *Scanning Probe Microscopy of Soft Matter: Fundamentals and Practices*. Wiley, 2011, pp 9-68.
- [11] G. Haugstad, *Atomic force microscopy: understanding basic modes and advanced applications*. Wiley, 2012, pp. 1-90.
- [12] Agilent Technologies. *Understanding the Fundamental Principles of Vector Network Analysis: Application Note* [online]. USA, 2012. Available: <http://cp.literature.agilent.com/litweb/pdf/5965-7707E.pdf>
- [13] Agilent Technologies. *Network Analyzer Basics* [online].USA, 2004. Available: <http://cp.literature.agilent.com/litweb/pdf/5965-7917E.pdf>
- [14] Agilent Technologies. *Introduction to Scanning Microwave Microscopy Mode: Application Note* [online]. USA, 2009. Available: https://www.chem.agilent.com/Library/applications/AN-IntroSMM_5989-8881.pdf
- [15] A. V. Tikhonravov, M. K. Trubetskov, J. Hrdina et al. "Characterization of quasi-rugate filters using ellipsometric measurements", *Thin Solid Films*, vol. 277, no. 1-2, pp. 83–89, 1996.
- [16] Agilent Technologies. *Agilent PicoView Software Enhanced Imaging and Analysis Package for Agilent AFM Systems: Data Sheet* [online]. USA, 2012. Available: <http://cp.literature.agilent.com/litweb/pdf/5991-1175EN.pdf>
- [17] H. Vašková, "Raman spectroscopy as an innovative method for material identification", Recent Researches in Automatic Control - 13th WSEAS International Conference on Automatic Control, Modelling and Simulation, ACMOS'11, 2011, pp. 292-295.
- [18] F. Hruška, "Electromagnetic interference and environment", *International Journal of Circuits, Systems and Signal Processing*, 8, 2014, pp. 22-29.
- [19] Lazar, J. et al., "Multiaxis interferometric system for positioning in nanometrology", 9th WSEAS International Conference on Microelectronics, Nanoelectronics, Optoelectronics, MINO '10, 2010, pp. 92-95.